



## Modeling, Control and Simulation of a High-Current DC-DC Converter for Fuel Cell Applications

H. Y. Kanaan<sup>1</sup>, S. Georges<sup>2</sup>, I. Mougharbel<sup>3</sup>, N. Mendalek<sup>2</sup> and T. Nicolas<sup>1</sup>

<sup>1</sup> Department of Electricity and Mechanics

Saint-Joseph University, Faculty of Engineering - ESIB

Campus des Sciences et Technologies, Mar Roukoz, Mkalles, B.P. 11-0514 – Beirut 1107 2050 (Lebanon)

Phone numbers: +961 3 333179, +961 3 480551, e-mails: [hadi.kanaan@fi.usj.edu.lb](mailto:hadi.kanaan@fi.usj.edu.lb), [tony.nicolas@fi.usj.edu.lb](mailto:tony.nicolas@fi.usj.edu.lb)

<sup>2</sup> Department of Electrical Engineering

Notre-Dame University (NDU), P.O. Box 72 – Zouk Mosbeh (Lebanon)

Phone numbers: +961 3 716461, +961 3 163693, e-mails: [sgeorges@ndu.edu.lb](mailto:sgeorges@ndu.edu.lb), [nmendalek@ndu.edu.lb](mailto:nmendalek@ndu.edu.lb)

<sup>3</sup> Department of Electrical Engineering

Lebanese University, Faculty of Engineering – Hadath (Lebanon)

Phone number: +961 3 315373, e-mail: [imadmoug@ul.edu.lb](mailto:imadmoug@ul.edu.lb)

**Abstract.** In this paper, a high-current two-stage DC-DC converter fed by a Proton Exchange Membrane Fuel Cell (PEMFC) is studied. The converter consists of two three-phase full-bridge inverters connected through three AC coupled inductors. The mathematical models of both converter and PEMFC are first presented, and a control scheme that ensures a high power factor at the AC stage and a regulated voltage at the DC load is then implemented. The performance of the proposed control system is verified through digital simulations.

### Key words

DC-DC converter, three-phase inverters, six-switch rectifiers, fuel cells, high currents, modeling, control.

### 1. Introduction

During the last two decades, several DC-DC topologies that cover a wide power range have been proposed. Most of them, based on the use of MOSFETs, were dedicated to low power applications, and are generally provided with a high frequency transformer that ensures galvanic isolation at the mid-stage. In addition, the input stage of such converters is limited to a two-leg inverter, whereas the output stage consists only of rectifying diodes, yielding thus a unidirectional power flow.

In high current applications, the use of two-leg topologies becomes insufficient, and the extension to the above-mentioned converters to the three-phase case becomes mandatory due to the limited ratings of the available semiconductors [1]. Furthermore, in order to decrease the current ratings in such converters without affecting the power level, a high power factor is required at the AC mid-stage. This feature makes necessary the replacement

of the conventional diode bridge output stage by a fully controlled six-switch rectifier. This topological modification will have other advantages: 1) the power flow becomes now bi-directional, 2) the regulation of the DC voltage at the rectifier output becomes possible, 3) the power losses in the copper and the magnetic core are reduced, which is due essentially to the reduction of the RMS-currents and the elimination of low-frequency current harmonics, 4) the power efficiency is consequently increased, 5) the size, weight and cost of the magnetic core are reduced, and 6) the EMI disturbances become negligible.

The DC-DC topology considered in this paper is described in Fig. 1. It is used to connect a Proton Exchange Membrane Fuel Cell (PEMFC) to a DC load at different voltage level. The converter consists of two six-switch inverters connected through three AC inductors coupled on a same magnetic core. The bulkiness of the magnetic core could be easily and significantly reduced by increasing the fundamental frequency at the AC stage.

In this paper, mathematical models for the PEMFC source and DC-DC converter are presented, upon which a control scheme has been designed. Both six-switch bridges are controlled using the fixed-frequency carrier-based Pulse-Width-Modulation technique [2]. An open-loop control is applied to the inverter, whereas closed-loops current and voltage regulators are designed to control the rectifier on the basis of the state-space averaged model of the two-stage converter [3]. The proposed control system is tested through simulations for a resistive load, and the results have shown good performance regarding load voltage regulation and high power quality at the AC intermediate stage.

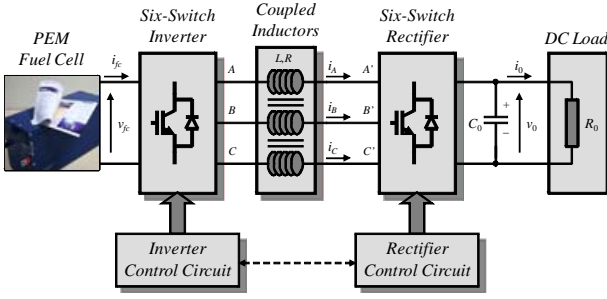


Fig. 1. Two-stage DC-DC converter for PEMFC

## 2. Modeling of the Power Stage

### A. PEMFC Model

Based on the work presented in [4], a PEMFC stack can be modeled as illustrated in Fig. 2. The stack output voltage  $v_{fc}$  is expressed in terms of the cell current  $i_{fc}$  and the stack parameters as follows:

$$v_{fc} = E - R_{fc} i_{fc} = E_{oc} - NA \ln \left( \frac{i_{fc}}{i_0} \right) \cdot \frac{1}{T_d s + 1} - R_{fc} i_{fc} \quad (1)$$

$$E_{oc} = NE_n \quad (2)$$

where  $R_{fc}$  denotes the stack resistance,  $E_{oc}$  the open circuit voltage,  $N$  the number of cells in series,  $E_n$  the Nernst voltage,  $A$  the Tafel slope,  $i_0$  the exchange current and  $T_d$  the fuel cell response time.

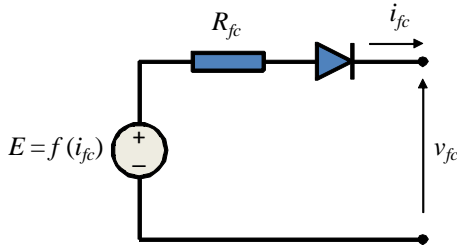


Fig. 2. PEMFC stack model.

### B. State-Space Average Model of the DC-DC Converter

According to [3], the state-space average model of the two-stage DC-DC converter is given as:

$$L \frac{di_d}{dt} = -R i_d + L \omega i_q + d_d v_{fc} - d'_d v_0 \quad (3)$$

$$L \frac{di_q}{dt} = -R i_q - L \omega i_d + d_q v_{fc} - d'_q v_0 \quad (4)$$

$$C_0 \frac{dv_0}{dt} = \frac{3}{2} (d'_d i_d + d'_q i_q) - \frac{v_0}{R_0} \quad (5)$$

where  $i_d$  and  $i_q$  represent respectively the  $d$ -axis and  $q$ -axis components of currents  $i_A$ ,  $i_B$  and  $i_C$  in the synchronous frame,  $v_0$  is the DC-load voltage,  $d_d$  and  $d_q$  are respectively the  $d$ -axis and  $q$ -axis components of the duty cycles corresponding to the inverter upper switches, expressed in the synchronous frame,  $d'_d$  and  $d'_q$  are respectively the  $d$ -axis and  $q$ -axis components of the duty

cycles corresponding to the rectifier upper switches, expressed in the synchronous frame,  $R_0$  and  $R$  represent respectively the DC load and power losses in each AC-side inductor, and  $\omega$  is the angular frequency at the intermediate AC stage.

## 3. Control System

### A. Inverter Control

The three system outputs are all controllable by operating only the output stage rectifier. In this case, the inverter control becomes quite simple, and would consist only of an open loop gate signals generation using the conventional sine-triangle pulse-width-modulation technique. Hence, by denoting  $u_A$ ,  $u_B$  and  $u_C$  the inverter reference signals defined as:

$$\begin{aligned} u_A(t) &= \hat{u} \cdot \sin(\omega t) \\ u_B(t) &= \hat{u} \cdot \sin(\omega t - 2\pi/3) \\ u_C(t) &= \hat{u} \cdot \sin(\omega t - 4\pi/3) \end{aligned} \quad (6)$$

which would be compared to a common high-frequency triangular carrier with a peak value  $\hat{v}_{tri}$ , the expressions of the duty cycles that correspond to the inverter upper switches become in the stationary frame:

$$\begin{aligned} d_A(t) &= \frac{1}{2} + \frac{r}{2} \sin(\omega t) \\ d_B(t) &= \frac{1}{2} + \frac{r}{2} \sin(\omega t - 2\pi/3) \\ d_C(t) &= \frac{1}{2} + \frac{r}{2} \sin(\omega t - 4\pi/3) \end{aligned} \quad (7)$$

and in the rotating frame:

$$\begin{aligned} d_d &= \frac{r}{2} \\ d_q &= 0 \\ d_0 &= \frac{3}{2} \end{aligned} \quad (8)$$

where  $r = \hat{u}/\hat{v}_{tri}$  denotes the voltage regulation parameter, and  $d_0$  the zero-sequence component of inverter upper switches duty cycles.

Furthermore, in order to minimize the current constraints at rated power consumption, the parameter  $r$  is set to its maximum value  $r_{max} = 1$ .

### B. Rectifier Control

A multiple-loops linear control system is designed for the rectifier using the averaged model in the rotating frame given in section 2.B. The control scheme is presented in Fig. 3.  $\mathbf{K}$  represents the stationary/synchronous frame transformation. The current references  $i_d^*$  and  $i_q^*$  are generated as follows [3]:



simulations. It was shown that the converter exhibits high operation quality in term of mid-stage current distortion and power factor.

## Appendix

### A. PEMFC Parameters

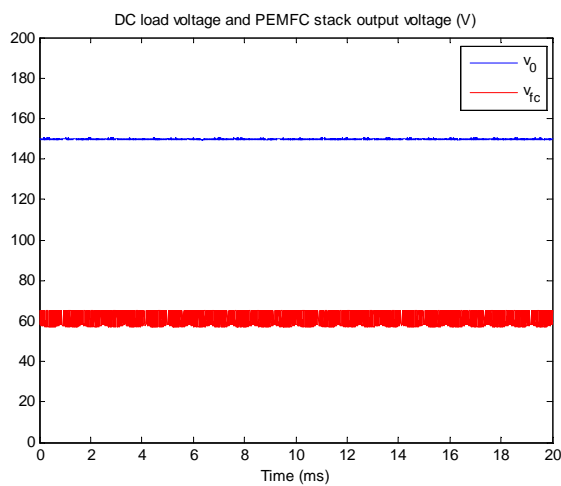
Open circuit voltage	$E_{oc} = 65 \text{ V}$
Number of cells in series	$N = 65$
Nernst voltage	$E_n = 1 \text{ V}$
Tafel slope	$A = 30.7 \text{ mV}$
Exchange current	$i_0 = 0.94 \text{ A}$
Fuel cell response time	$T_d = 10 \text{ s}$
Stack resistance	$R_{fc} = 75.8 \text{ m}\Omega$

### B. DC-DC Converter and Control System Parameters

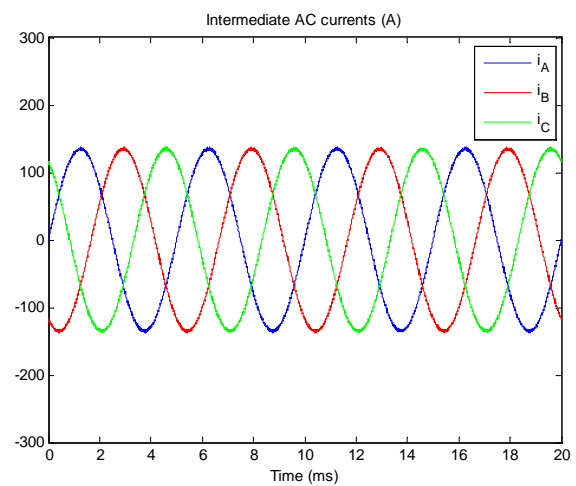
Desired DC load voltage	$v_0^* = 150 \text{ V}$
Nominal load power	$P = 6 \text{ kW}$
Fundamental frequency	$f = \omega/2\pi = 200 \text{ Hz}$
Switching frequency	$f_s = 20 \text{ kHz}$
AC-side inductors	$L = 100 \mu\text{H}$ , each
DC-side capacitor	$C_0 = 1 \text{ mF}$
Feedback scaling gains	$K_i = K_v = 1$

$$\text{Inner regulators} \quad H_{i,d}(s) = H_{i,q}(s) = -\frac{s+45}{s}$$

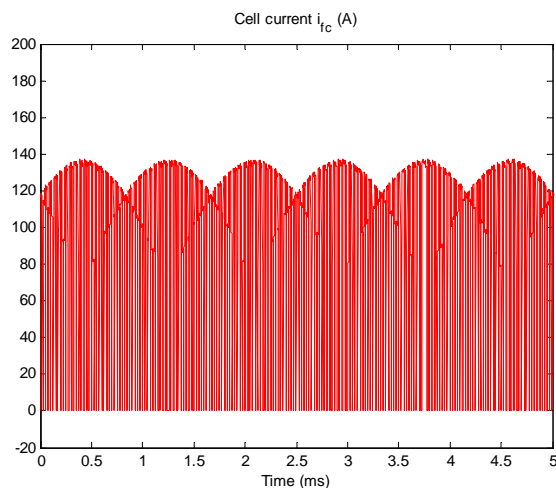
$$\text{Outer regulator} \quad H_v(s) = 3\frac{s+1}{s}$$



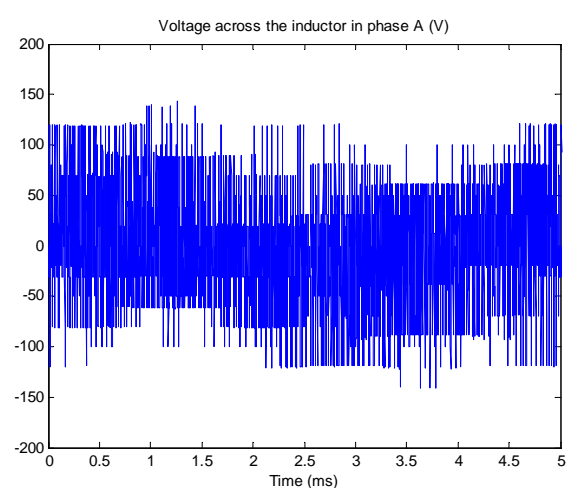
(a)



(b)

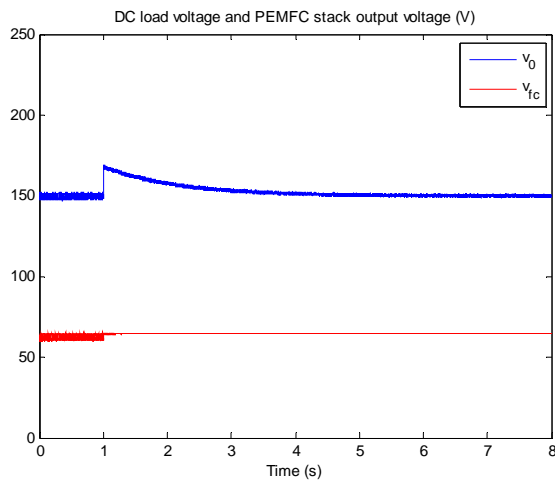


(c)

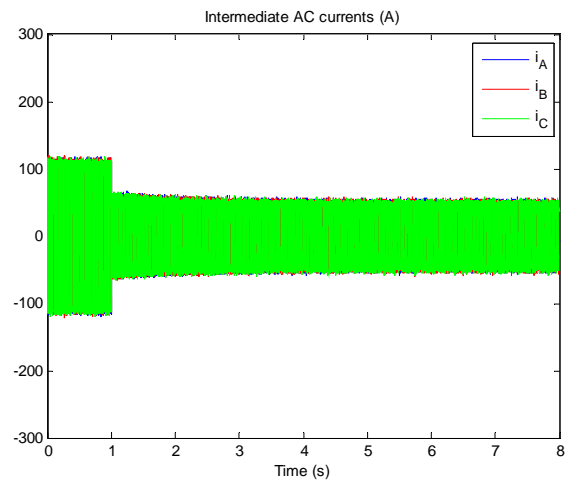


(d)

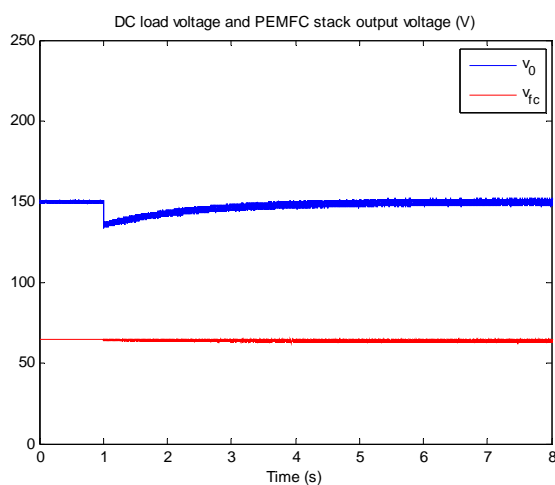
Fig. 5. Steady-state waveforms of (a) the DC load voltage and the PEMFC stack output voltage, (b) the AC mid-stage currents, (c) the cell current and (d) the voltage across the inductor in phase A.



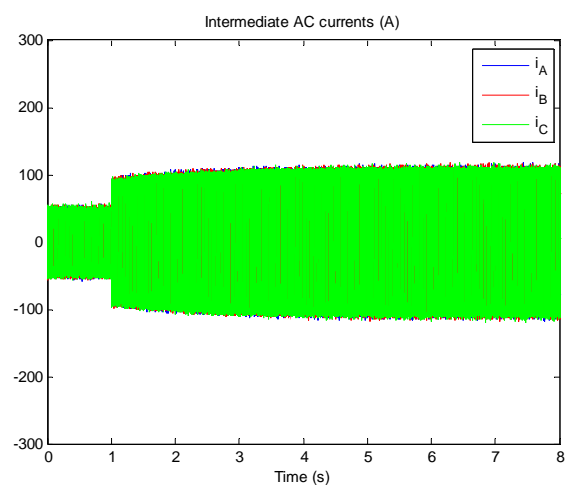
(a)



(b)



(c)

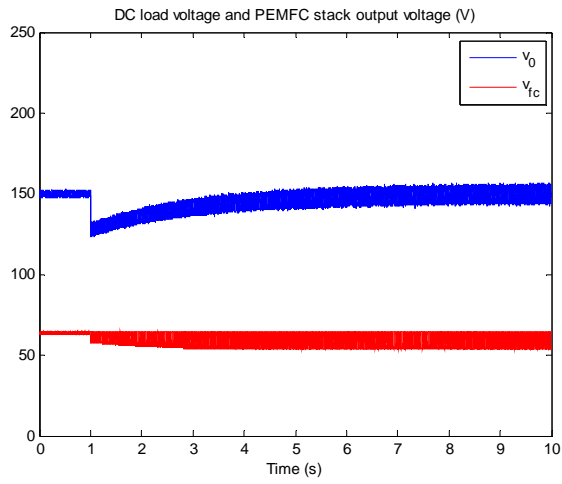


(d)

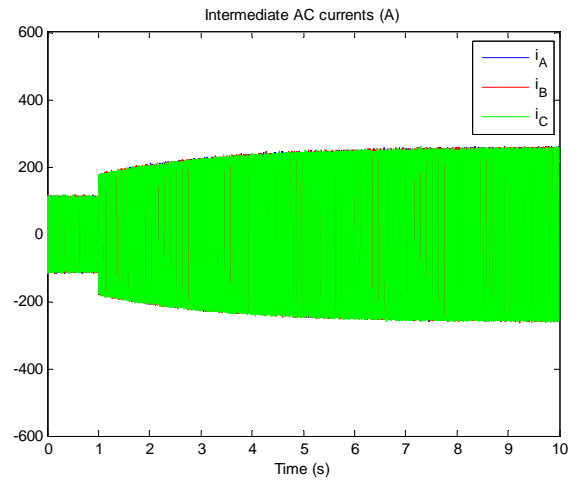
Fig. 6. Impacts of a load step decrease (from 6kW to 3kW) and increase (from 3kW to 6kW) on the DC load voltage and the PEMFC stack output voltage (Figs. 6.a and 6.c respectively), and on the AC mid-stage currents (Figs. 6.b and 6.d respectively).

## References

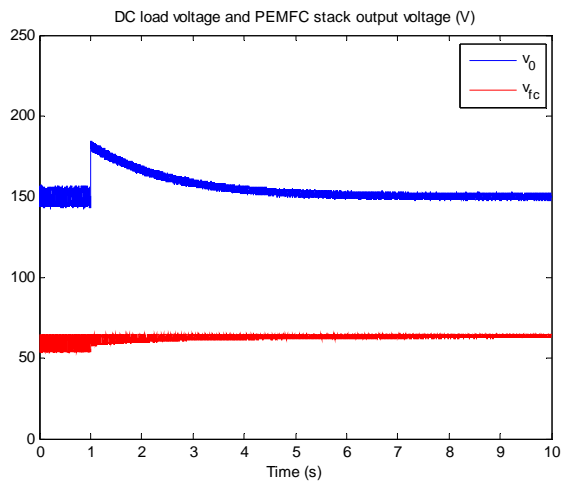
- [1] J. Jacobs, A. Averberg and R. De Doncker, "A novel three-phase DC/DC converter for high-power applications", *35th Ann. IEEE Power Electr. Spec. Conf. (PESC'04)*, Aachen, Germany, 1992, pp.1861-1867.
- [2] R. Wu, S. B. Dewan and G. R. Slemon, "Analysis of an AC-to-DC voltage source converter using PWM with phase and amplitude control", *IEEE Trans. Ind. Applic.*, vol.27, No.2, pp. 355-364, Mar./Apr. 1991.
- [3] H. Y. Kanaan and K. Al-Haddad, "Design, control and simulation of a high-efficiency low-cost DC-DC converter for high current applications", in *Proc. 28<sup>th</sup> International Telecommunications Energy Conference (INTELEC'06)*, Providence, Rhode Island, USA, September 10-14, 2006, pp. 1-8.
- [4] S. Njoya Motapon, "A Generic Fuel Cell Model and Experimental Validation", *Ecole de Technologie Supérieure*, Montréal, Canada, Département de Génie Electrique, Mémoire de Maîtrise, June 2008.
- [5] J. M. Maciejowski, *Multivariable Feedback Design*, Addison-Wesley, 1989.
- [6] [www.fuelcellmarkets.com/content/images/articles/ps6.pdf](http://www.fuelcellmarkets.com/content/images/articles/ps6.pdf)
- [7] H. Y. Kanaan, S. Abourida, A. Hayek and K. Al-Haddad, "Switching-functions-based state-space modeling and simulation of a two-stage high power DC-DC converter", in *Proc. 2<sup>nd</sup> International Conference on Modeling, Simulation and Applied Optimization (ICMSAO'07)*, Abu Dhabi, UAE, March 24-27, 2007.



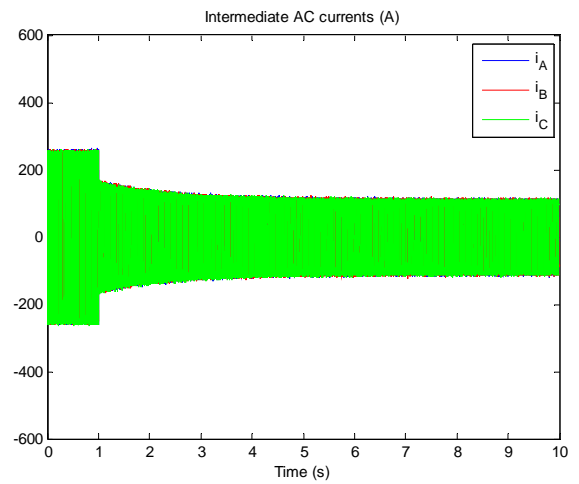
(a)



(b)



(c)



(d)

Fig. 7. Impacts of a load step increase (from 6kW to 12kW) and decrease (from 12kW to 6kW) on the DC load voltage and the PEMFC stack output voltage (Figs. 7.a and 7.c respectively), and on the AC mid-stage currents (Figs. 7.b and 7.d respectively).